Combined viscous and dry friction damping of oscillatory motion

Peter F. Hinrichsen and Chris I. Larnder
John Abbott College, Sainte Anne de Bellevue, Quebec H9X 3L9, Canada

(Received 10 November 2017; accepted 9 April 2018)

The acceleration, velocity, and displacement of a glider on an air track undergoing oscillatory motion subject to viscous and dry frictional damping are investigated using an accelerometer, which allowed a detailed investigation of the dynamics, experimental observation of the predicted acceleration discontinuities due to the reversal of the friction force, and the variation of the drag with time, velocity, and displacement. The investigation included systematic variation of the air track air pressure to explicitly control the relative contribution of viscous and dry frictional damping. Although frictional damping of oscillatory motion has been treated by a number of authors, most investigations have been restricted to measurements of displacement only, with the primary interest being in the decay of the amplitude. In this paper, an exact theory of the acceleration of oscillatory motion, assuming viscous damping proportional to the velocity plus a Coulomb friction force independent of velocity or position, is presented and compared with experiment.
https://doi.org/10.1119/1.5034345

I. INTRODUCTION

There is a rich literature on the damping of oscillatory motion as this was an important correction to early precision pendulum clocks[1] and measurements of the earth's gravity.[2] Introductory texts almost universally treat the damping of oscillatory motion as proportional to the velocity, as the resulting differential equation can be simply solved, leading to an exponential decay and a period dependent on the damping but independent of the amplitude.[3–6] This theory provides a convenient analog to LCR circuits, and can be extended to treat the resonance response of these systems.[7] For real mechanical systems, this is generally an oversimplification and it has been shown by Stokes[8] (see Ref. 9) that the damping of a pendulum in air was larger than calculated. However, the difference between the damping in air and in vacuum agreed well with the calculated air damping. Thus, the remaining damping could be assigned to damping by the friction in the suspension system, i.e., making and breaking of micro welds at the suspension points, which accounted for about half of their damping. Understanding the damping of the motions of the pendular suspensions of the LIGO mirrors is important in optimization of the sensitivity to gravitational waves.[10]

The damping of oscillatory motion with dry (i.e., Coulomb) friction,[11–33] viscous[11–16,30,34–39] (i.e., proportional to velocity) and quadratic[7,9,11,12,40–45] drag have been investigated by many authors. However, for dry frictional damping the concentration has been on demonstrating the linear decay of the amplitude, determining the final rest position[17,18,29] and the coefficients of friction. The equation of motion, assuming kinetic friction independent of velocity or position and equal to the maximum static friction, is easily solved for successive half oscillations using a change of variable,[46] trial functions[11] or using the work-energy theorem,[31] and has also been solved using Laplace transforms.[19,23] The approximate solution due to Wang,[12] however, does not include the displacement offset from the equilibrium position.

Den Hartog[47] was the first to solve the periodic sliding response of a harmonically forced oscillator with a model of both viscous and frictional damping. Markho[48] published the first derivation of the equation for the amplitude decay curve (or envelope) for such a system vibrating freely under no-stop conditions. Squire[11] and Vitorino[31] have presented approximate solutions for combined quadratic, viscous and frictional damping; however, their solutions, although correctly reproducing the amplitude decay, do not include the offset from the equilibrium position or acceleration discontinuities. Ricchiuto and Tozzi[49] present the theory for the decay of the amplitude and the present paper extends the theory to cover the acceleration.

Measurements of the acceleration of the damped oscillatory motion of a glider on an air track as a function of the air track air pressure are reported and fall into four categories. At normal operating air track air pressure the drag on the glider, for large amplitude oscillations, was found to have viscous[35] plus a small quadratic component. However, as the air track air pressure is reduced, i.e., the air film is reduced in width, the viscous drag proportional to velocity predominates. At lower air track air pressures, when the glider only partially floats and touches the track, the drag is a combination of viscous and frictional components, with friction dominating at the lowest air track pressure.

The acceleration data were integrated to derive the velocity and the displacement. Least-squares fits of the theory reproduced the general features of the acceleration and displacement data, which then allowed the nature of the drag force to be directly investigated. It is well known that the Coulomb theory is only an approximation, which does not include striction, the transition from static to dynamic friction and other effects,[20] so the present theory is not expected to describe all details of the motion.

II. THEORY OF COMBINED VISCOUS AND COULOMB FRICTION DAMPING

The friction force F_f parallel to the contact surface is assumed to be independent of velocity or position[22,50] and such as to oppose the motion. Then for a mass m attached to a spring of spring constant k, subject to both Coulomb friction F_f, and a viscous damping force $F(\dot{x}) = -b\dot{x}$ proportional to velocity, the equation of motion is

$$m\ddot{x} = -kx - b\dot{x} - F_f Sgn(\dot{x})$$
$$\ddot{x} + 2\alpha\dot{x} + \omega_o^2(x + \Delta x Sgn(\dot{x})) = 0 \quad (1)$$

where $\omega_o^2 = k/m$, $\alpha = b/2m = 1/\tau_\alpha$ and $Sgn(\dot{x}) = 1, 0, -1$ for $\dot{x} > 0, \dot{x} = 0, \dot{x} < 0$, i.e., the friction force always opposes the motion, changing sign at the turning points in x, see Fig. 1. In addition, $\Delta x = F_f/k$ is the magnitude of the displacement at which the friction force just equals the spring force, thus for initial displacements $|x| \leq \Delta x$ the spring force cannot overcome the friction and no oscillation occurs.

The discontinuity in the friction force requires each half oscillation to be treated separately, as is also the case for a precise treatment of quadratic damping.[44] Changing the variable to $\chi = (x \pm \Delta x)$ for each half oscillation, the equation becomes the standard equation $\ddot{\chi} + 2\alpha\dot{\chi} + \omega_o^2\chi = 0$ for viscously damped harmonic motion with $\chi = (x - \Delta x)$ for $\dot{x} \leq 0$ and $\chi = (x + \Delta x)$ for $\dot{x} \geq 0$. For release from rest with $x(0) = x_o$, $\dot{x}(0) = 0$ the solution is $\chi(t) = (\omega_o/\omega)\chi_o \exp(-\alpha t)\cos\omega(t - t_\alpha)$ with $\omega^2 = \omega_o^2 - \alpha^2$ and the phase ωt_α given by $\tan\omega t_\alpha = \alpha/\omega$. So for the first half oscillation,[6] i.e., $n = 0$, the velocity is negative and the offset Δx is positive. Then for this first half oscillation

$$x(t) = \frac{\omega_o}{\omega}(x_0 - \Delta x)e^{-\alpha t}\cos\omega(t - t_\alpha) + \Delta x$$
$$\dot{x}(t) = -\frac{\omega_o^2}{\omega}(x_0 - \Delta x)e^{-\alpha t}\sin\omega t$$
$$\ddot{x}(t) = -\frac{\omega_o^3}{\omega}(x_0 - \Delta x)e^{-\alpha t}\cos\omega(t + t_\alpha)$$
$$\dddot{x}(t) = \frac{\omega_o^4}{\omega}(x_0 - \Delta x)e^{-\alpha t}\sin\omega(t + 2t_\alpha). \quad (2)$$

Although the displacement maxima and velocity zeros occur at times $nT/2$, i.e., the times at which the friction reverses, the acceleration maxima occur $2t_\alpha$ before the velocity zeros, see Fig. 1.

At $t = T/2$, i.e., after the first half oscillation, the displacement has a minimum, the velocity is zero and the friction force reverses. Thus, the displacement $x(T/2)$ at the end of the first half oscillation, which is $x(T/2) = (-1)^1\{x_o e^{-\alpha t/2} - \Delta x(1 + e^{-\alpha t/2})\} = x_1(T/2)$, equals

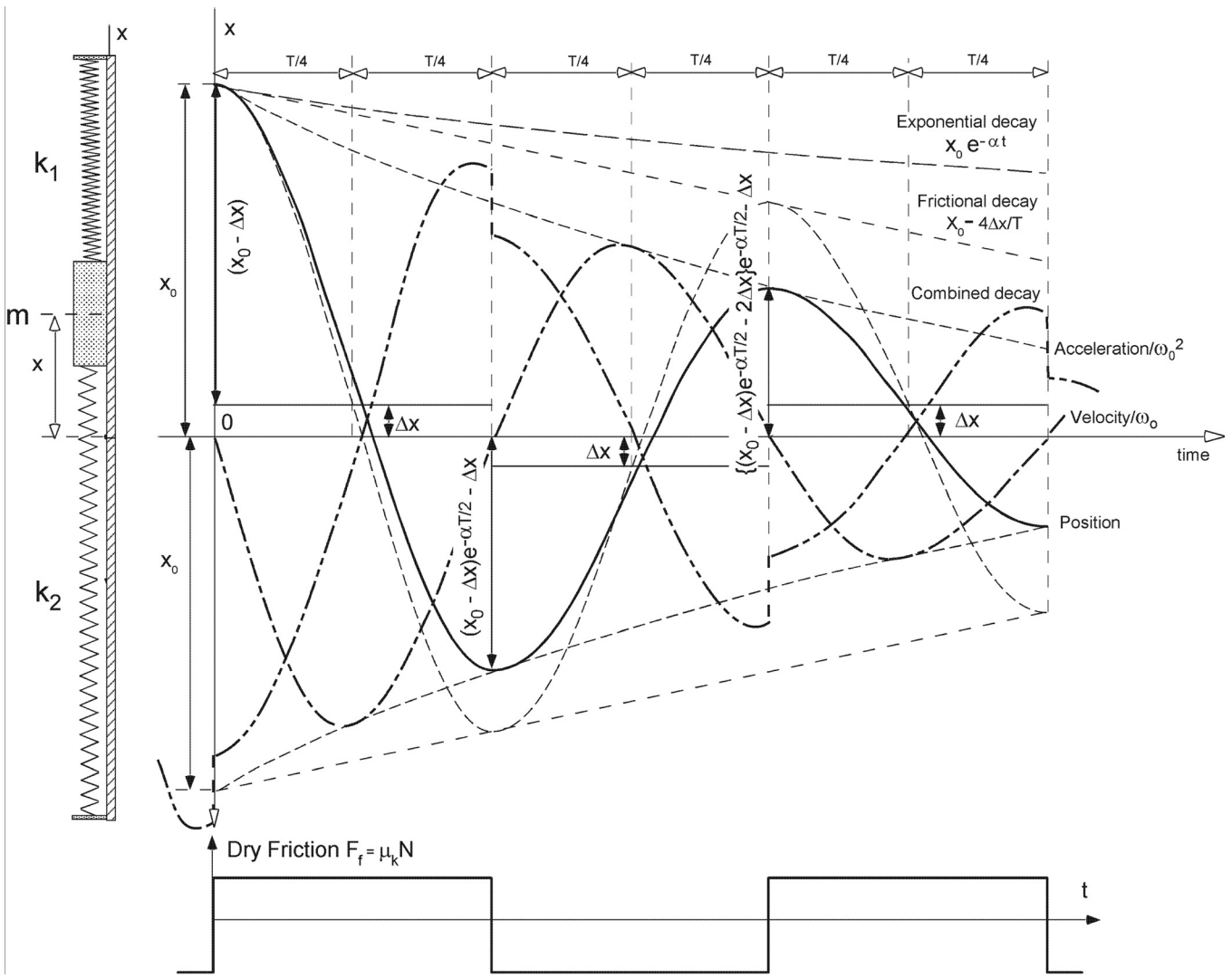

Fig. 1. The decay of oscillatory motion with viscous plus Coulomb friction damping, displacement (solid line), velocity/ω_0, (dotted-dashed), and acceleration/ω_0^2 (double dotted-dashed). The labelled dashed lines represent the amplitude decay curves for (i) viscous damping only, (ii) Coulomb friction only, and (iii) both terms combined.

the initial displacement $x_1(T/2)$ for the second half oscillation. Similarly, the displacement at the end of the second half oscillation is the initial displacement for the third half oscillation $x_1(T)=(-1)^2\{x_o[e^{-\alpha t/2}]^2-\Delta x(1+2e^{-\alpha t/2}+[e^{-\alpha t/2}]^2)\}$ $=x_2(T)$. This can then be generalized as a geometric series, beginning with the first half oscillation $n=0$. The displacement at the beginning of the nth half oscillation, i.e., the displacement maxima, is then

$$\begin{aligned} x_n(nT/2) = x_n &= (-1)^n\{x_o\beta^n - \Delta x(1+2\beta \\ &\quad + 2\beta^2\cdots+2\beta^{n-1}+\beta^n)\} \\ x_n &= (-1)^n\left\{x_o\beta^n - \Delta x\frac{(1+\beta)(1-\beta^n)}{(1-\beta)}\right\}, \end{aligned} \tag{3}$$

where $\beta = e^{-\alpha T/2}$ is the amplitude decay per half oscillation due to viscous drag. In contrast to the displacement maxima as given in Eq. (3), the initial amplitude of the nth half oscillation section is

$$A_n = |x_n| - \Delta x = \left\{x_o\beta^n - \Delta x\frac{(2-\beta^n(1+\beta^n))}{(1-\beta)}\right\} \tag{4}$$

with this oscillation being about an equilibrium position displaced by $(-1)^n\Delta x$. Then substituting the amplitude A_n into Eq. (2) and noting that the offset Δx changes sign every half oscillation, the displacement, velocity, and acceleration are given by

$$\begin{aligned} x_n(t) &= \frac{\omega_o}{\omega}\left\{x_o - \Delta x\frac{(2\beta^{-n}-(1+\beta))}{(1-\beta)}\right\}e^{-\alpha t} \\ &\quad\times\cos\omega(t-t_\alpha) + (-1)^n\Delta x \\ \dot{x}_n(t) &= -\frac{\omega_o^2}{\omega}\left\{x_o - \Delta x\frac{(2\beta^{-n}-(1+\beta))}{(1-\beta)}\right\}e^{-\alpha t}\sin\omega t \\ \ddot{x}_n(t) &= -\frac{\omega_o^3}{\omega}\left\{x_o - \Delta x\frac{(2\beta^{-n}-(1+\beta))}{(1-\beta)}\right\}e^{-\alpha t} \\ &\quad\times\cos\omega(t+t_\alpha) \end{aligned} \tag{5}$$

with acceleration "discontinuities" of $\Delta\ddot{x} = 2\omega_o^2\Delta x = 2F_f/m$ occurring at the zero velocity times. Note that the displacement is continuous, as the section amplitude change is offset by the change in the equilibrium position, and the velocity is continuous as velocity amplitude changes when the velocity is zero. This solution predicts that the period is independent of the frictional damping and the amplitude, i.e., it is the same as the period for viscous damping, and that the amplitude decays until it reaches the stagnation interval $-\Delta x \le x_n(nT/2) \le \Delta x$. The treatment of quadratic damping also involves matching piecewise solutions for half oscillations[45] and could therefore be incorporated into the above analysis.

For pure viscous damping, i.e., $F_f=0$, Eq. (3) reduces to the well-known exponential decay of the amplitude, while for pure friction damping, i.e., $\alpha=0$, Eq. (5) becomes

$$\begin{aligned} x(t) &= \{x_o - (2n+1)\Delta x\}\cos\omega_o t + (-1)^n\Delta x \\ \dot{x}(t) &= -\omega_o\{x_o - (2n+1)\Delta x\}\sin\omega_o t \\ \ddot{x}(t) &= -\omega_o^2\{x_o - (2n+1)\Delta x\}\cos\omega_o t. \end{aligned} \tag{6}$$

This linear dependence of the amplitude on the half oscillation number n follows directly from Eq. (6), or alternatively from work energy as applied to a half oscillation, $(k/2)(x_n^2 - x_{n+1}^2) = F_f(x_n - x_{n+1})$, namely, the loss in potential energy, for motion from maximum to minimum displacement, equals the work done by the friction force. Hence the amplitude decrease each half oscillation is $|x_n + x_{n+1}| = 2F_f/k = 2\Delta x$, which is in agreement with Eq. (6), and this can be extended to include viscous damping.[31]

For combined viscous and frictional damping the successive acceleration values at zero velocity,[51] see Eq. (5), facilitate the separation of the contributions to the damping, which are given by

$$\Delta x = \frac{(-1)^n(\ddot{x}_{n+1}\ddot{x}_{n-1} - \ddot{x}_n^2)}{\omega_0^2(\ddot{x}_{n+1} - \ddot{x}_{n-1})} \quad \alpha = \frac{2}{T}ln\left(-\frac{\ddot{x}_{n-1}+\ddot{x}_n}{\ddot{x}_n+\ddot{x}_{n+1}}\right). \tag{7}$$

Finally, Eq. (1) can be reformulated as

$$\xi = \frac{\ddot{x}}{\omega_o^2} + x = -\frac{2\alpha}{\omega_o^2}\dot{x} - \Delta x Sgn(\dot{x}) = -\frac{b\dot{x}+F_f}{k} = -\frac{F_D}{k}, \tag{8}$$

where the parameter ξ is the total drag force divided by the spring constant k. It can be derived from the acceleration, displacement and period, and allows the nature of the drag force to be directly extracted from the data. A graph of ξ versus the velocity $\dot{x}$ theoretically leads to a linear plot of slope $-(2\alpha/\omega_o^2)$, from which α can be determined, and a discontinuity of $2\Delta x$ at zero velocity. Such an analysis facilitates a detailed investigation of the dissipative mechanisms, reveals asymmetries and deviations from the simple model of friction, and is much more sensitive than a simple inspection of the amplitude decay, see, for example, Figs. 8 and 9.

III. EXPERIMENTAL PROCEDURE

The measurements were made with a glider of mass 634.3 gm, length 288 mm, with 59 mm wide sides at 90°, floating on a 1.65 m-long air track. Two similar springs of initial length of 65 and 85 mm and masses 7.07 and 11.65 gm, respectively, were attached to the glider and track ends. The effective spring constant of the springs was 2.96 N/m, as determined from the variation of the glider equilibrium position as a function of the track inclination angle, leading to a predicted oscillation period of $T = 2.91 \pm 0.02$ s. Unfortunately some hysteresis in the springs limited the precision of these measurements.

The glider acceleration was measured by a Gulf Coast[52] GCX2-2 (sensitivity 0.74 m/s^2 per count at 512 Hz) accelerometer, which was mounted on the side of the glider

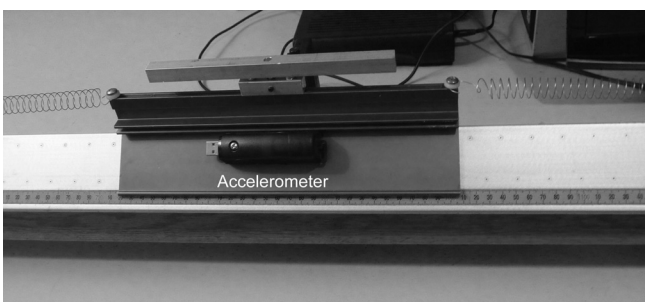

Fig. 2. The air track glider with the two springs attached to it and the GCX6-2 accelerometer mounted on it.

with the x axis parallel to the track, see Fig. 2. The air track air pressure, as measured by a water manometer, was varied from 4.74 kPa, for which the glider floats free, to 0.79 kPa at which the frictional drag was dominant. For each run the initial displacement from the equilibrium position was 400 mm.

The acceleration data from the GCX2-2 were first corrected for offset and drift,[53] using data with the glider stationary before and after oscillation. The velocity and position, with appropriate choice of initial values, were then calculated by numerical integration and further corrected for drift. The acceleration data exhibited a small parasitic 20 Hz oscillation and were therefore averaged over 0.05 s intervals to eliminate this and reduce the noise. The data with frictional and viscous damping were analysed in two ways. First, Eq. (5) was modelled in Excel and the solver routine used to fit the model to the acceleration data. The period T, initial amplitude x_0, frictional decrement Δx and damping constant α, were fitted by least-squares minimization. Finally, in order to examine the drag force in detail, $\xi = (\ddot{x}/\omega_o^2 + x)$, i.e., the drag force divided by the spring constant, was calculated and compared with the theory.

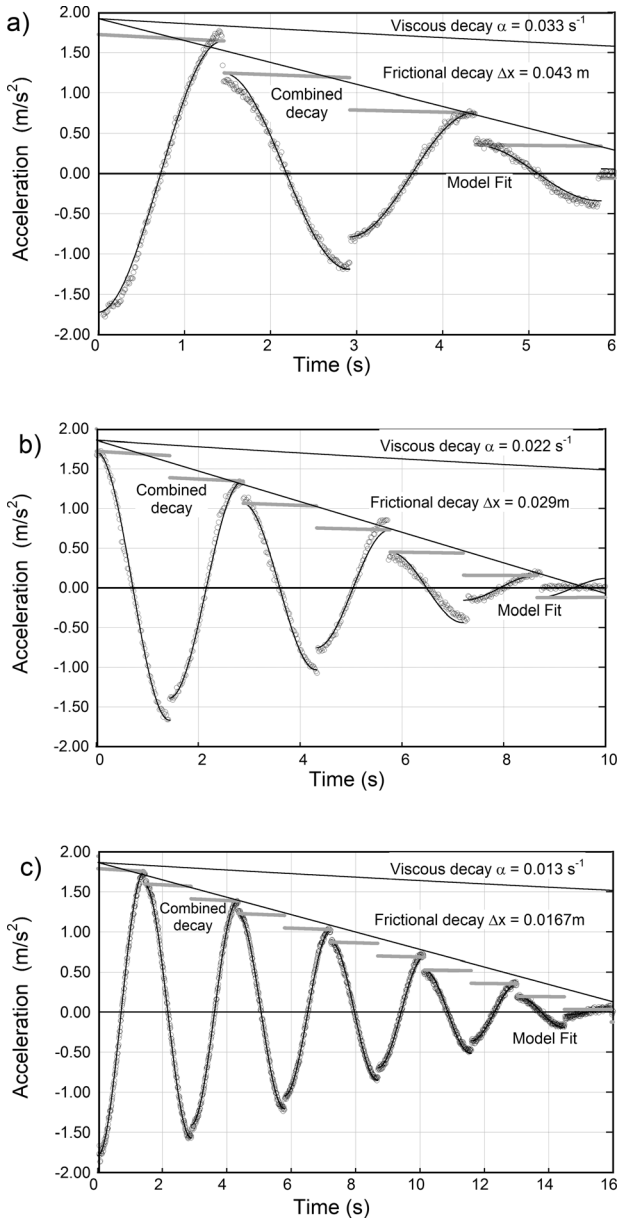

Fig. 3. The glider acceleration as a function of time (s) at air track pressures of (a) 0.79 kPa, (b) 0.86 kPa, and (c) 0.90 kPa. The combined decay is a combination of the frictional and viscous decay as derived from the model fit. For clarity in this and subsequent figures only one in five acceleration data points, open circles, are plotted. Note: for (b) the glider was released from a negative initial displacement.

IV. RESULTS

In order to establish the properties of the system without dry frictional drag, measurements were made with air track air pressures between1.07 kPa and 4.74 kPa for which the amplitude decay was essentially exponential, with time constants between 200 s and 300 s, plus some indication of

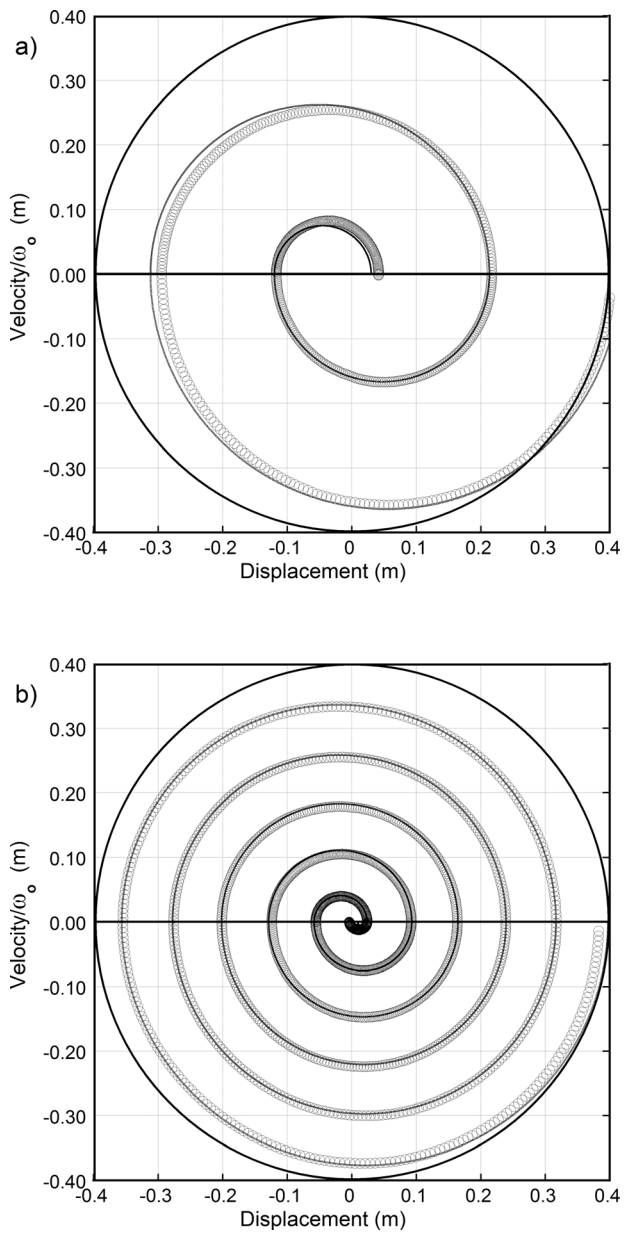

Fig. 4. Phase plots of the velocity/ω_0 versus the displacement, data open circles, and Eq. (5) model solid points, for the oscillations with air track pressure (a) 0.79 kPa and (b) 0.90 kPa. In the absence of damping the motion would lead to the circumscribing circles shown. Note that the velocity is continuous.

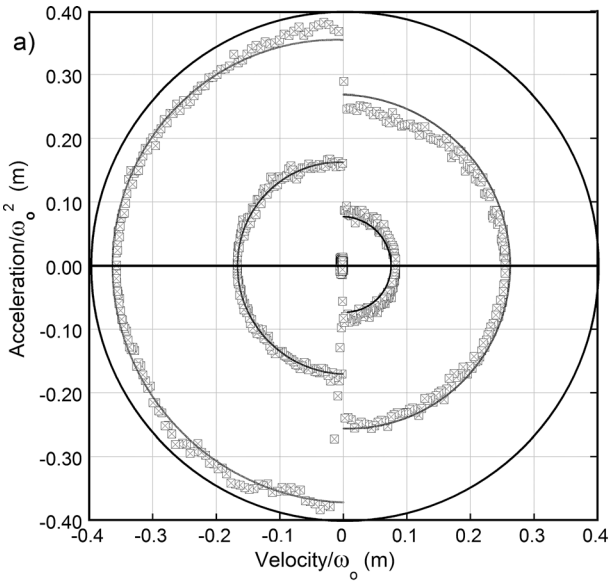

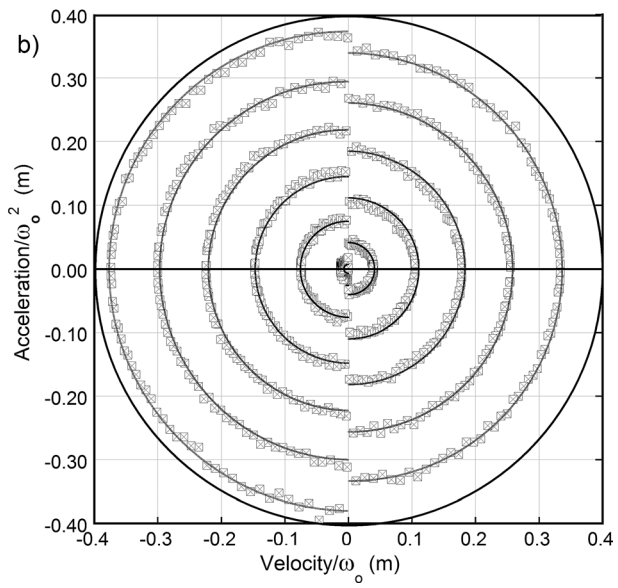

Fig. 5. Plots of the acceleration/$\omega_0{}^2$ versus the velocity/ω_0, data open squares, and Eq. (5) model solid points, for the oscillations with air track air pressure (a) 0.79 kPa and (b) 0.90 kPa, demonstrating the acceleration discontinuities at zero velocity. In the absence of damping the motion would lead to the circumscribing circles shown.

quadratic damping[9] at large amplitudes. The data at air track air pressures between 0.79 kPa and 0.90 kPa, see Fig. 3, clearly show the discontinuities in the acceleration due to friction reversal at the position turning points. However, the acceleration amplitude does not decay linearly, thus indicating that there is both frictional and viscous damping present. The fits to Eq. (5) reproduce the observed acceleration discontinuities and the amplitude decay; however, contrary to the model prediction, the individual acceleration discontinuities are not of equal magnitude, as can be more clearly seen in Fig. 8.

The data derived from the accelerometer are of sufficient precision for it to be presented in a number of instructive ways. Phase plots of the velocity/ω_0 versus the displacement, together with fits of Eq. (5) are shown in Figs. 4(a) and 4(b) and demonstrate the continuous decay of the velocity. Figures 5(a) and 5(b) provide similar plots of the

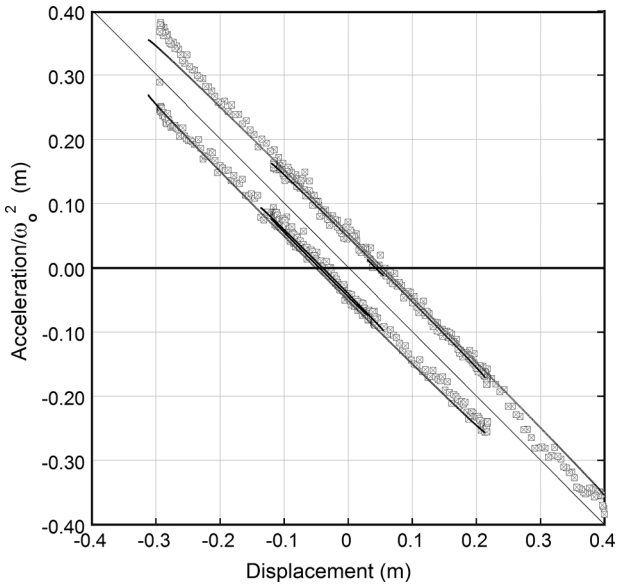

Fig. 6. Plot of the acceleration/$\omega_0{}^2$ vs the displacement, data open squares, and Eq. (5) model solid points, for the oscillations with air track air pressure 0.79 kPa, demonstrating the shift in the displacement for zero acceleration with the direction of the velocity. In the absence of damping, the motion would lead to the straight diagonal line through the origin.

acceleration/$\omega_0{}^2$ versus the velocity/ω_0, and clearly illustrates the acceleration discontinuities at zero velocity. For $\alpha/\omega \ll 1$, Eq. (5) leads to $\ddot{x}(t)/\omega_o^2 \approx -x(t) + (-1)^n \Delta x$, so a plot of the acceleration/$\omega_0{}^2$ versus the displacement should have a slope of -1 with offsets of $\pm\Delta x$ and this is illustrated in Fig. 6, which shows the plus and minus offsets Δx from the equilibrium position when the acceleration is zero.

The total energy $E(t) = m/2\{\dot{x}^2 + \omega_o^2 x^2\}$, together with the kinetic and potential energies, are shown as functions of the time, and of the displacement in Figs. 7(a) and 7(b), respectively. The non-uniform rate of energy loss[15,30,54,55] can be clearly seen, with maximum energy loss rate when the velocity is at a maximum, and zero loss rate when the velocity is zero. The almost linear energy loss with displacement[18] is illustrated in Fig. 7(b). Equation (5) is a good fit except for the first half oscillation, and this may be due to start up transients affecting the drag and/or quadratic damping.

A. Analysis of the drag force $F_D = -k\xi$

The total drag force F_D can be extracted from the data as $F_D = -k(\ddot{x}/\omega_o^2 + x) = -k\xi$, thus plots of ξ, i.e., the drag force divided by the spring constant, can provide information on the nature of the drag force and its dependence on the velocity and displacement. It must be pointed out that ξ is the difference between the magnitudes $|\ddot{x}/\omega_o^2|$ and $|x|$, and therefore these quantities must be precisely determined, which is much easier with integration of acceleration data than from differentiating position data. Adding the acceleration/$\omega_0{}^2$ to the smooth displacement data, i.e., calculating ξ is analogous to calculating the acceleration residuals (which would be zero for SHM) and can reveal the presence of dry friction long before it is evident in the amplitude decay. The variation of ξ with time is shown in Fig. 8 together with the acceleration data and the model drag as deduced from the fit of Eq. (5). It can be seen that at 0.79 kPa the model is a good fit, except again for the first half oscillation. At an air track

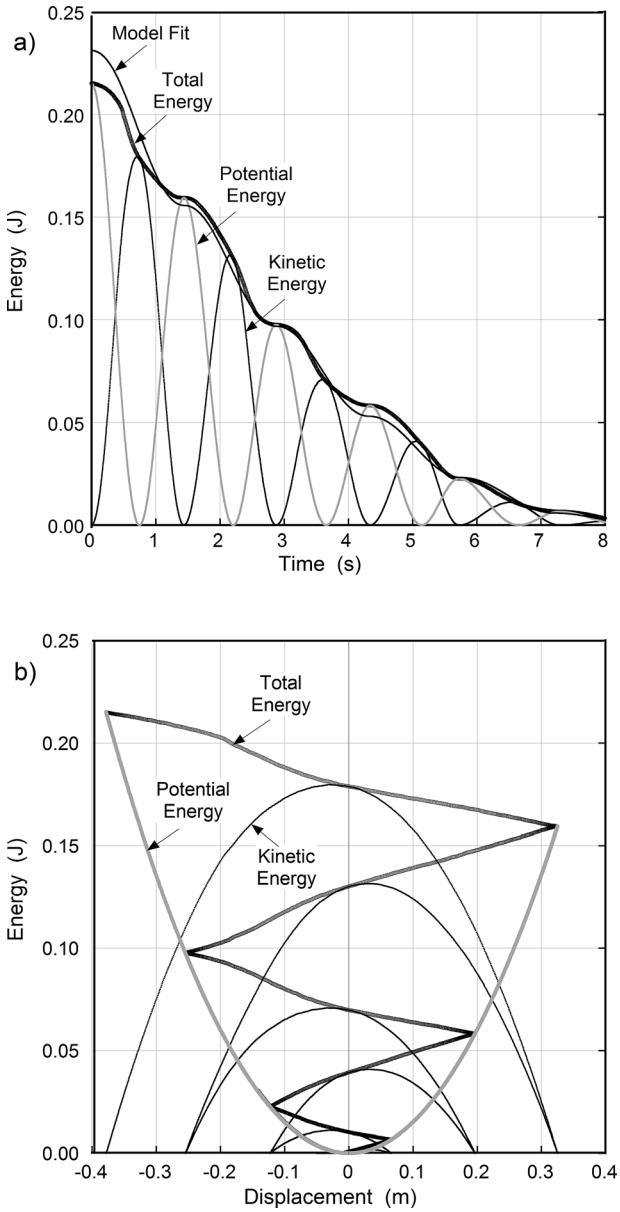

Fig. 7. Plots versus (a) time and (b) displacement of the total energy data, heavy points, potential energy data, gray points, and kinetic energy data, light points, for an air track air pressure of 0.86 kPa. The Eq (5) model fit is shown in (a). Note that, as shown in (b), the maximum kinetic energy does not occur at zero displacement.

air pressure of 0.86 kPa, the drag force is seen to vary significantly and Fig. 9(a), a plot of ξ versus displacement, indicates that there was an increase in the drag at displacements around -0.1 m. Figure 9(b) clearly shows the non-uniform drag discontinuities at zero velocity, and also indicates that the drag was direction-dependent. Subsequent examination of the air track revealed that it was not perfectly linear, thus introducing a small cubic term into the potential and presumably affecting the glider interaction with the track and the friction as a function of position.

V. CONCLUSIONS

The present experiments are an extension of the classical undergraduate studies of simple harmonic motion on an air track, but with the significant advantage that an accelerometer was used to record the motion. In order to study the effects of combined viscous and frictional damping, these forces were varied by reducing the air track air pressure in a controlled manner. The recorded acceleration of the damped oscillatory motion was of sufficient precision that, in the presence of dry friction, the acceleration discontinuities at the zero velocity points could be clearly observed experimentally.

The velocity and displacement were derived by simple numerical integration, which smoothed the data and allowed a wide variety of aspects of this motion to be studied in greater detail than was previously possible.

The theory of combined viscous and simple Coulomb friction damping of oscillatory motion including the acceleration has been derived and shown to reproduce the essential features of the experimental data. The present exact theory is essentially similar to that of Ricchiuto and Tozzi[49] but is extended to include the acceleration. It reproduces the acceleration discontinuities and the alternating offset of the equilibrium position, which previous approximate theories[11,31] were not able to do.

The analysis of the acceleration and displacement to extract the drag force has been used to confirm that the model is a good first approximation, but also revealed that the practical situation is more complex than this model, i.e., the drag force was also a function of the displacement and was direction dependent. Adding the displacement data to the acceleration/ω_0^2 data is somewhat akin to calculating the acceleration residuals, and is therefore a sensitive way of analysing oscillatory data. Such an analysis should allow the

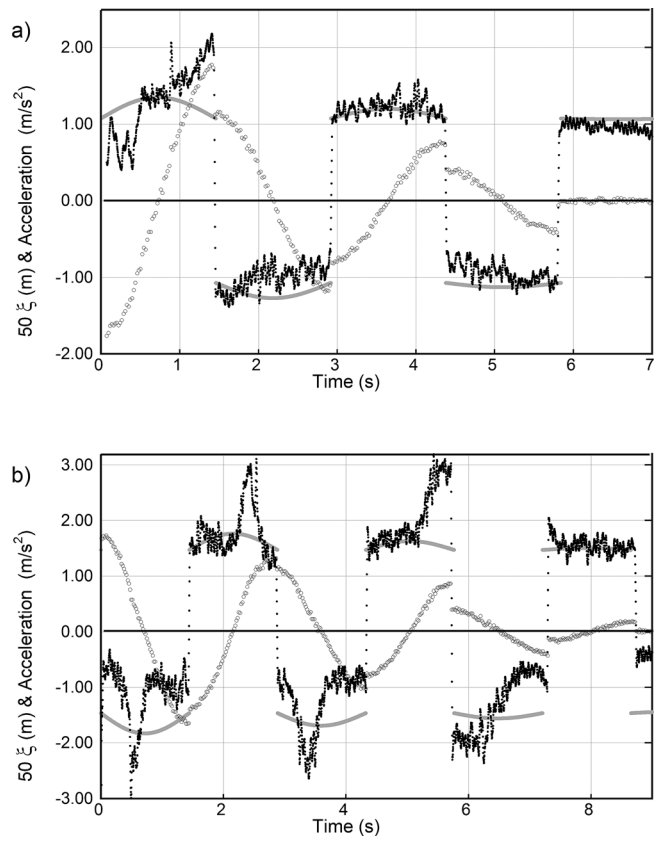

Fig. 8. Plots of the acceleration, open circles and (a) 50xξ data, solid points, and the Eq. (5) model, gray points, at an air track air pressure of 0.79 kPa vs time. (b) 50xξ data, and the Eq. (5) model, at an air track pressure of 0.86 kPa. Note that the acceleration discontinuities are not uniform.

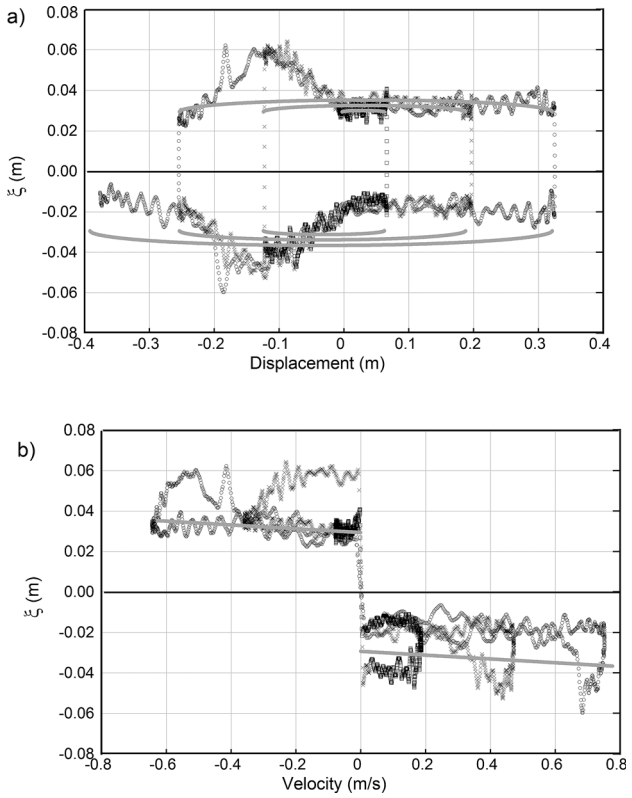

Fig. 9. Plot of ξ data (first oscillation open circles, second crosses and third open squares) and the Eq. (5) model, gray points, versus (a) displacement and (b) velocity, at an air track pressure of 0.86 kPa. Note the consistently larger values around a displacement of −0.1 m and the difference for positive and negative velocities.

nature of the damping effects in more complex situations to be studied as functions of velocity and displacement, and is a much more stringent test than the usual analysis of only the amplitude decay.[9,11]

The many student experiments on harmonic motion[6,7,11,12,15,16,29] that in the past measured displacement can now be performed using accelerometers[39] or gyroscopes, as these are generally available in most smartphones and inexpensively provide precision data. The present measurements were made with an air track and commercial accelerometer, however, they can be made with smartphones, with low friction cart systems,[15,30,56,57] or pendula.[11]

A number of experimental investigations of dry friction damping of oscillatory motion have been published and could usefully use accelerometers. However, student experiments generally emphasize linear damping, which can be enhanced by the use of magnets,[6] but most laboratory equipment is nevertheless subject to some frictional drag, which with the precision now available, is likely be observed by students. It is therefore of interest to have an exact theory available, even if combined viscous and frictional drag is not a part of the curriculum.

ACKNOWLEDGMENTS

The accelerometer was purchased with a grant from the Entente Canada-Quebec.

[1]P. Woodward, *Woodward on Time: A Compilation of Philip Woodward's Horological Writings* (Bill Taylor, British Horological Institute, 2006).
[2]A. H. Cook, "A new absolute determination of the acceleration due to gravity at the National Physical Laboratory, England," Philos. Trans. A **261**(1120), 211–252 (1967).
[3]S. T. Thornton and J. B. Marion, *Classical Dynamics of Particles and Systems* (Thompson Brooks Cole, Belmont, CA, 2004).
[4]G. L. Baker and J. A. Blackburn, *The Pendulum a Case Study in Physics* (Oxford U.P., Oxford, 2005).
[5]R. D. Gregory, *Classical Mechanics*, First ed. (Cambridge U.P., Cambridge, 2006).
[6]P. F. Hinrichsen, "Acceleration, velocity and displacement for damped SHM," Phys. Teach., (submitted).
[7]A. Li, L. Ma, D. Keene, J. Klingel, M. Payne, and X.-J. Wang, "Forced oscillations with linear and nonlinear damping," Am. J. Phys. **84**(1), 32–37 (2016).
[8]G. G. Stokes, "On the effect of the internal friction of fluids on the motion of pendulums," Trans. Camb. Philos. Soc. **IX**, 8–94 (1850).
[9]R. A. Nelson and M. G. Olsson, "The pendulum-rich physics from a simple system," Am. J. Phys. **54**(2), 112–121 (1986).
[10]T. Findley, S. Yoshida, and D. P. Norwood, "Analysis of the pendular and pitch motions of a driven three-dimensional pendulum," Eur. J. Phys. **28**, 331–340 (2007).
[11]P. T. Squire, "Pendulum damping," Am. J. Phys. **54**(11), 984–991 (1986).
[12]X.-J. Wang, C. Schmitt, and M. Payne, "Oscillations with three damping effects," Eur. J. Phys. **23**(2), 155–164 (2002).
[13]M. I. Molina, "Exponential versus linear amplitude decay in damped oscillators," Phys. Teach. **42**(8), 485–488 (2004).
[14]J. C. Simbach and J. Priest, "Another look at a damped physical pendulum," Am. J. Phys. **73**(11), 1079–1080 (2005).
[15]M. D'Anna, P. Lubini, M. Marhl, and V. Grubelnik, "The energy of a damped oscillator", in *GIREP-EPEC Frontiers of Physics Education* (Opatija, Croatia, 2007), pp. 1–5.
[16]G. Torzo and P. Peranzoni, "The real pendulum: theory, simulation, experiment," Lat. Am. J. Phys. Educ. **3**(2), 221–228 (2009); PACS: 06.50, 07.10, 46.30P ISSN 1870-9095.
[17]I. R. Lapidus, "Motion of a harmonic oscillator with sliding friction," Am. J. Phys. **38**(11), 1360–1361 (1970).
[18]I. R. Lapidus, "Motion of a harmonic oscillator with variable sliding friction," Am. J. Phys. **52**(11), 1015–1016 (1984).
[19]R. C. Hudson and C. R. Finfgeld, "Laplace transform solution for the oscillator damped by dry friction," Am. J. Phys. **39**(5), 568–570 (1971).
[20]P. R. Dahl, "Solid friction damping of mechanical vibrations," AIAA J. **14**(12), 1675–1682 (1976).
[21]C. Barratt and George L. Strobel, "Sliding friction and the harmonic oscillator," Am. J. Phys. **49**(5), 500–501 (1981).
[22]R. D. Peters and Tim Pritchett, "The not-so-simple harmonic oscillator," Am. J. Phys. **65**(11), 1067–1073 (1997).
[23]C. Pelto, K. Coates, and N. Jaggi, "Harmonic oscillation in the presence of multiple damping forces" Honors Projects. Paper 1, Illinois Wesleyan University http://digitalcommons.iwu.edu/physics_honproj/1, 1997.
[24]L. F. C. Zonetti, A. S. S. Camargo, J. Sartori, D. F. de Sousa, and L. A. O. Nunes, "A demonstration of dry and viscous damping of an oscillating pendulum," Eur. J. Phys. **20**(2), 85–88 (1999).
[25]L. M. Burko, "A piecewise-conserved constant of motion for a dissipative system," Eur. J. Phys. **20**(4), 281–288 (1999).
[26]M. B. Ottinger, "Harmonic oscillator damped by sliding friction," in Transactions of the Missouri Academy of Science (https://www.thefreelibrary.com/Harmonic+oscillator+damped+by+sliding+friction.-a0103376624, 2002).
[27]A. Marchewka, D. S. Abbott, and R. J. Beichner, "Oscillator damped by a constant-magnitude friction force," Am. J. Phys. **72**(4), 477–483 (2004).
[28]M. Kamela, "An oscillating system with sliding friction," Phys. Teach. **45**(2), 110–113 (2007).
[29]P. Onorato, D. Mascoli, and Anna De Ambrosis, "Damped oscillations and equilibrium in a mass-spring system subject to sliding friction forces: Integrating experimental and theoretical analyses," Am. J. Phys. **78**(11), 1120–1127 (2010).
[30]T. Corridoni, M. D'Anna, and H. Fuchs, "Damped mechanical oscillator: experiment and detailed energy analysis," Phys. Teach. **52**(2), 88–90 (2014).
[31]M. V. Vitorino, A. Vieira, and M. S Rodrigues, "Effect of sliding friction in harmonic oscillators," Sci. Rep. **7**(1), 3726–3731 (2017).
[32]L. Cveticanin, "Analyses of oscillators with non-polynomial damping terms," J. Sound Vib. **317**(3–5), 866–882 (2008).

[33]L. Cveticanin, "Oscillators with nonlinear elastic and damping forces," Comput. Math. Appl. **62**(4), 1745–1757 (2011).
[34]V. K. Gupta, G. Shanker, and N. K. Sharma, "Experiment on fluid drag and viscosity with an oscillating sphere," Am. J. Phys. **54**(7), 619–622 (1986).
[35]B. S. Andereck, "Measurement of air resistance on an air track," Am. J. Phys. **67**(6), 528–533 (1999).
[36]Daniel Hoyt, "More on damped oscillators," Phys. Teach. **43**(4), 196–197 (2005).
[37]R. D. Peters, "Nonlinear damping of the 'linear' pendulum," preprint arXiv:physics/0306081 (2003).
[38]S. Shamim, W. Zia, and Muhammad Sabieh Anwar, "Investigating viscous damping using a webcam," Am. J. Phys **78**, 433–436 (2010).
[39]J. C. Castro-Palacio, L. Velazquez, M. H. Gimenez, and J. A. Monsoriu, "Using the mobile phone acceleration sensor in Physics experiments: Free and damped harmonic oscillations," Am. J. Phys. **81**(6), 472–475 (2013).
[40]F. S. Crawford, "Damping of a simple pendulum," Am. J. Phys. **43**(3), 276–277 (1975).
[41]M. F. McInerney, "Computer-aided experiments with the damped harmonic oscillator," Am. J. Phys. **53**(10), 991–996 (1985).
[42]L. Basano and Pasquale Ottonello, "Digital pendulum damping: the single-oscillation approach," Am. J. Phys. **59**(11), 1018–1023 (1991).
[43]C. E. Mungan and Trevor C. Lipscombe, "Oscillations of a quadratically damped pendulum," Eur. J. Phys. **34**, 1243–1253 (2013).
[44]L. Cveticanin, "Oscillator with strong quadratic damping force," Publ. L'Institute Math. **85**(99), 119–130 (2009).
[45]B. R. Smith, Jr., "The quadratically damped oscillator: A case study of a non-linear equation of motion," Am. J. Phys. **80**(9), 816–824 (2012).
[46]E. I. Butikov, "Torsion spring oscillator with dry friction," <butikov.faculty.ifmo.ru/Applets/DryFrictionNL.pdf> (2013), pp. 1–21.
[47]J. P. Den Hartog, "Forced vibrations with combined viscous and coulomb damping," Trans. Am. Soc. Mech. Eng. **53**, 107–115 (1930).
[48]P. H. Markho, "On free vibrations with combined viscous and coulomb damping," J. Dyn. Syst. Meas. Control **102**(4), 283–286 (1980).
[49]A. Ricchiuto and A. Tozzi, "Motion of a harmonic oscillator with sliding and viscous friction," Am. J. Phys. **50**(2), 176–179 (1982).
[50]E. I. Butikov, *Simulations of Oscillating Systems, with award-winning software* (CRC Press, Taylor & Francis Group, Boca Raton, 2015).
[51]Z. Wu, H. Lui, L. Lui, and D. Yuan, "Identification of nonlinear viscous damping and Coulomb friction from the free response data," J. Sound Vib. **304**(1–2), 407–414 (2007).
[52]Gulf Coast, USB Accelerometer Model GCX2-2 <www.gcdataconcepts.com> (2010).
[53]J. R. Evans, R. M. Allen, A. I. Chung, E. S. Cochran, R. Guy, M. Hellweg, and J. F. Lawrence, "Performance of several low-cost accelerometers," Seismological Res. Lett. **85**(1), 147–158 (2014).
[54]I. Grigore, C. Miron, and E. S. Barna, "Exploring the graphic facilities of Excel spreadsheets in the interactive teaching and learning of damped harmonic oscillations," Romanian Rep. Phys. **68**(2), 891–904 (2016); available at rrp.infim.ro/IP/A70.pdf.
[55]E. A. Karlow, "Ripples in the energy of a damped harmonic oscillator," Am. J. Phys. **62**, 634–636 (1994).
[56]S. Egri and L. Szabó, "Analyzing oscillations of a rolling cart using smartphones and tablets," Phys. Teach. **53**(March), 161–163 (2015).
[57]Pasco Scientific, "Pasco Wireless Smart Cart ME-1240", in <https://www.pasco.com/file_downloads/Downloads_Manuals/Wireless-Smart-Cart-Manual-ME-1240-1.pdf>, edited by Pasco Scientific (10101 Foothills Blvd., Roseville, CA 95747-7100, 2016).

Jamin's Divided Circle

This is a generalized apparatus for making measurements of optical phenomena such as reflection, refraction and polarization. It can be equipped with a number of accessories, but in this example at the University of Vermont, it has a telescope arm and a collimator arm to allow it to be used as a spectrometer. If you look carefully, there is a circular table in the middle where a prism or diffraction grating can be placed. (Picture and Notes by Thomas B. Greenslade, Jr., Kenyon College)